

Modeling reflection spectra of super-Eddington X-ray sources

SWARNIM SHASHANK ¹, HONGHUI LIU ^{1,2}, ASKAR B. ABDIKAMALOV ^{3,1,4}, JIACHEN JIANG ^{5,6}, COSIMO BAMBI ^{1,3},
FERGUS BAKER,⁷ AND ANDREW YOUNG⁷

¹Center for Astronomy and Astrophysics, Center for Field Theory and Particle Physics and Department of Physics, Fudan University, Shanghai 200438, People's Republic of China

²Institut für Astronomie und Astrophysik, Eberhard-Karls Universität Tübingen, D-72076 Tübingen, Germany

³School of Humanities and Natural Sciences, New Uzbekistan University, Tashkent 100001, Uzbekistan

⁴Ulugh Beg Astronomical Institute, Tashkent 100052, Uzbekistan

⁵Institute of Astronomy, University of Cambridge, Madingley Road, Cambridge CB3 0HA, UK

⁶Department of Physics, University of Warwick, Gibbet Hill Road, Coventry CV4 7AL, UK

⁷School of Physics, University of Bristol, Tyndall Avenue, Bristol BS8 1TH, UK

ABSTRACT

We present a relativistic disk reflection model based on the geometry calculated using analytical formulae for super-Eddington accretion flows. This model features a slim disk geometry where the inner disk thickness is proportional to radius, becoming thicker as the mass accretion rate increases. The slim disk profile reduces the brightness of the blue horn in the Fe K emission line for a fixed emissivity and significantly changes the intensity profile for a lamppost geometry. The model is constructed assuming a spherically symmetric spacetime. It can be used for any kind of sources showing fluorescent reflection features and predicted to have slim accretion disks, like slow rotating black holes in X-ray binaries, active galactic nuclei, tidal disruption events, and neutron star X-ray binaries. To show the capability of the model, we use the 2017 *NICER* and *NuSTAR* data of the ultraluminous X-ray transient Swift J0243.6+6124.

Keywords: Accretion (14) — Ultraluminous x-ray sources (2164) — X-ray astronomy (1810)

1. INTRODUCTION

Super-Eddington accretion has become an important phenomenon to be studied in the recent years in sources where the luminosity exceeds the Eddington luminosity ($L_{\text{Edd}} \approx 1.26 \times 10^{38} M/M_{\odot} \text{ erg s}^{-1}$). It has been observed in Ultraluminous X-ray sources (ULXs) (Kaaret et al. 2017; Fabrika et al. 2021) which are compact objects observed in nearby galaxies and even one Galactic pulsar Swift J0243.6+6124 (Cenko et al. 2017; Kennea et al. 2017). Super-Eddington accretion has been observed in tidal disruption events (TDEs), which are transient events occurring when a star is disrupted (see Gezari 2021, for a recent review on TDEs) and accreted by a massive black hole (see Bloom et al. (2011);

Burrows et al. (2011); Kara et al. (2016, 2018); Lin et al. (2015)). There are also observations of super-Eddington accretion in active galactic nuclei (AGNs) (Lanzuisi et al. 2016; Tsai et al. 2018) where the accretion takes place onto supermassive black holes at the centres of galaxies. Accretion beyond the critical Eddington limit is also considered an important factor of growth of massive black holes discovered in the early Universe (Mortlock et al. 2011; Fan et al. 2023; Massoneau et al. 2023; Matthee et al. 2024).

Fluorescent iron lines are commonly observed in the X-ray spectra of a number of astrophysical sources, such as neutron star (Bhattacharyya & Strohmayer 2007; Cackett et al. 2008) and black hole (Tripathi et al. 2021; Draghis et al. 2023; Liu et al. 2023a) X-ray binaries (XRBs), AGNs (Nandra et al. 2007; Walton et al. 2013), and TDEs (Yao et al. 2022; Kara et al. 2016). The source of this emission line is predicted to be the “reflection” taking place at the accretion disk (or some optically thick medium). The Comptonized photons from hot

swarnim@fudan.edu.cn

Corresponding author: Cosimo Bambi
bambi@fudan.edu.cn

plasma around the central compact object interact with the material in the disk or outflow. This imprints the atomic data of the gas as emission and absorption lines onto the spectrum. However, due to the compact object there is strong gravity which blurs this reflection spectrum arising from gravitational redshift and Doppler boosting (see, e.g., [Bambi 2017](#); [Tanaka et al. 1995](#); [Fabian et al. 1989](#)). The relativistic reflection spectrum is characterized by the Compton hump and blurred elemental emission lines, out of which Fe K emission line at 6.4-6.9 keV is often the strongest feature ([Ross & Fabian 2005](#)). Studying these reflection features is termed as X-ray reflection spectroscopy (see, e.g., [Bambi et al. 2021](#)): it provides a useful tool to probe the accretion dynamics and gravitational effects near to the compact object and remains one of the leading techniques to measure black hole spins ([Brenneman & Reynolds 2006](#); [Draghis et al. 2023](#)) and even performing tests of fundamental physics ([Cao et al. 2018](#); [Tripathi et al. 2019](#)). However, the systematic effects introduced by the common assumption of a razor-thin accretion disk geometry ([Novikov & Thorne 1973](#); [Page & Thorne 1974](#)) have not been thoroughly investigated. Some studies (e.g., [Shashank et al. \(2022\)](#); [Jiang et al. \(2022\)](#); [Tripathi et al. \(2021\)](#); [Abdikamalov et al. \(2020\)](#); [Taylor & Reynolds \(2018\)](#)) have explored this topic, but they remain within the geometrically thin regime suitable for sub-Eddington accretion disks ($H/r \ll 1$). [Jiang et al. \(2022\)](#) found that the systematic uncertainty is small compared to the statistical uncertainty of current data. [Shashank et al. \(2022\)](#) studied these systematic uncertainties by fitting the data with the current reflection models to spectra obtained from numerically simulated disks and found that for current missions (*NuSTAR*) the models work well. Effects of geometrically thick disks were explored in [Riaz et al. \(2020a,b\)](#). Future high-resolution data from missions like AXIS, HEX-P, or Athena will require more precise models. This is particularly important in the super-Eddington regime, as more objects such as TDEs and ULXs exhibit relativistic reflection spectra in their X-ray observations (e.g., [Jaisawal et al. \(2019\)](#); [Yao et al. \(2022, 2024\)](#); [Kara et al. \(2016\)](#); [Motta et al. \(2017\)](#); [Veledina et al. \(2023\)](#)). A full model which takes into account slim disks for super-Eddington scenarios have not been developed for studying reflection spectra (as per the authors' knowledge). We note that there are indeed existing models for the thermal emissions arising from slim disk geometries ([Kawaguchi 2003](#); [Sadowski 2011](#); [Caballero-Garcia et al. 2017](#); [Wen et al. 2022](#)). Recently, [Zhang et al. \(2024\)](#) studied ironline emissions from the optically thick outflows in a super-Eddington regime.

In this work, we introduce a new relativistic reflection model based on a slim disk profile for super-Eddington accretion ([Watarai 2006](#)). The article is organised as follows. In Section 2, we describe the model REFLUX. Section 3 shows working of the model by fitting the *NICER* and *NuSTAR* data from the 2017 outburst of the galactic ULX pulsar Swift J0243.6+6124. Finally, we discuss the results and future directions in Section 4. Units used in this article are $G = c = 1$.

2. MODEL DESCRIPTION

To model the expected slim disk profile for a supercritical accreting source, we use the analytical disk model introduced by [Watarai \(2006\)](#). The model assumes an optically thick disk by introducing a radially dependent ratio $f = Q_{\text{adv}}^- / Q_{\text{vis}}^+$. Q_{adv}^- is the advective cooling rate and Q_{vis}^+ is the viscous heating rate (for their explicit forms, see [Watarai 2006](#)). f also depends on the accretion rate, which then controls the height of the disk in our implementation. The scale height of the disk is defined as

$$H = \left[(2N + 3) \frac{B\Gamma_{\Omega}\Omega_0^2}{\xi} \right]^{1/2} f^{1/2} \tilde{r}, \quad (1)$$

where Ω_0 is a multiplier to the Keplerian angular velocity ($\Omega = \Omega_0 \Omega_{\text{K}}$), which we set to unity for having a disk with Keplerian velocity (Ω_{K}), and $\Gamma_{\Omega} = -d \log \Omega / d \log r$ is the linear approximation form of the angular velocity. We take $B = 1$, $N = 3$, $\xi = 1.5$, and $\Gamma_{\Omega} = 1.5$ as detailed in [Watarai \(2006\)](#). f is defined as

$$f(x) = \frac{1}{2} \left[D^2 x^2 + 2 - Dx(D^2 x^2 + 4)^{1/2} \right], \quad (2)$$

where

$$D = \left[\frac{64\Omega_0^2}{(2N + 3)\xi B\Gamma_{\Omega}} \right]^{1/2}, \quad x = \frac{\tilde{r}}{\dot{m}}, \quad (3)$$

$\dot{m} = \dot{M} / \dot{M}_{\text{crit}}$ is the accretion rate in units of Eddington accretion rate ($\dot{M}_{\text{crit}} = L_{\text{Edd}}$, where L_{Edd} is the Eddington luminosity of the source), and \tilde{r} is the disk radius. In our implementation of the model, we only vary \dot{m} , which gives us a family of disks whose scale heights are controlled by the value of \dot{m} . Also, we keep the inner edge of the disk as a free parameter, hence the \tilde{r} represented above is the disk radius starting from the inner edge. Fig. 1 shows the disk profile obtained by changing the value of the accretion rate.

To construct a full relativistic reflection model, we assume Schwarzschild spacetime around the central object. Further we use the same methods of ray-tracing ([Abdikamalov et al. 2024a](#)) and Cunningham's transfer

function (Cunningham 1975; Speith et al. 1995; Dauser et al. 2010) as demonstrated in detail in Bambi et al. (2017); Abdikamalov et al. (2019, 2020) (specifically, exactly the same methods have been used to calculate the transfer functions as discussed in Sec. 3 of Abdikamalov et al. (2020) for a thin disk with finite thickness).

The free parameters of the model are: the inner edge of the disk, which in the current version of REFLUX varies from $6M$ to $500M$, the accretion rate, which is varied from $1\dot{M}_{\text{crit}}$ to $100\dot{M}_{\text{crit}}$, and the inclination of the disk, varying from 3° to 70° . While constructing the model, we also have the outer radius of the disk up to $1000M$. For the lamppost versions, we have the height of the lamppost corona ranging from $2.2M$ to $100M$. With higher values of inclination, the photons from the inner regions of the disk do not reach the distant observer, so we do not consider inclinations higher than 70° . In Fig. 2, we show the variations in iron line profiles for different parameter values, we see that the thickness of the disk produces a change in the shape of the ironlines, reducing the blue horn from thinner to a thicker disk. Fig. 3 shows the ironline profiles for a lamppost emissivity. In the lamppost corona geometry, the emissivity profile of the disk significantly changes as inner region of the disk is more illuminated due to the thicker disk. For low corona heights and high accretion rates, the outer regions of the disk are shadowed due to the thickness of the disk.

REFLUX works along with the `xillver` (García et al. 2013) tables for calculating the reflection spectra in the rest frame of the gas. Tab. 1 guides the full set of parameters available across the different sub-models (flavors) of REFLUX¹. Each of the sub-model mainly arises from using different `xillver` tables. Sub-models with LP suffix mean they use a lamp-post emissivity. REFLUX is the base model using the angle-resolved cutoff power-law `xillver` table. REFLUXCp uses the `xillverCp` table with `nthComp` (Zdziarski et al. 1996; Życki et al. 1999) Comptonization for incident spectrum. REFLUXD uses the `xillverD` table, which has electron density as a free parameter and cutoff power-law with energy cutoff of 300 keV. RELLINE_SD is the relativistic line model.

3. SPECTRAL FITTING OF A ULX PULSAR

In this section, we discuss the results of our fitting we obtained for the Galactic ULX pulsar Swift J0243.6+6124 (Cenko et al. 2017; Kennea et al.

¹ With the exception of \dot{m} which is the accretion rate, the parameters listed in Tab. 1 are same as that of the `relxill` model listed here: <https://www.sternwarte.uni-erlangen.de/~dauser/research/relxill/index.html>.

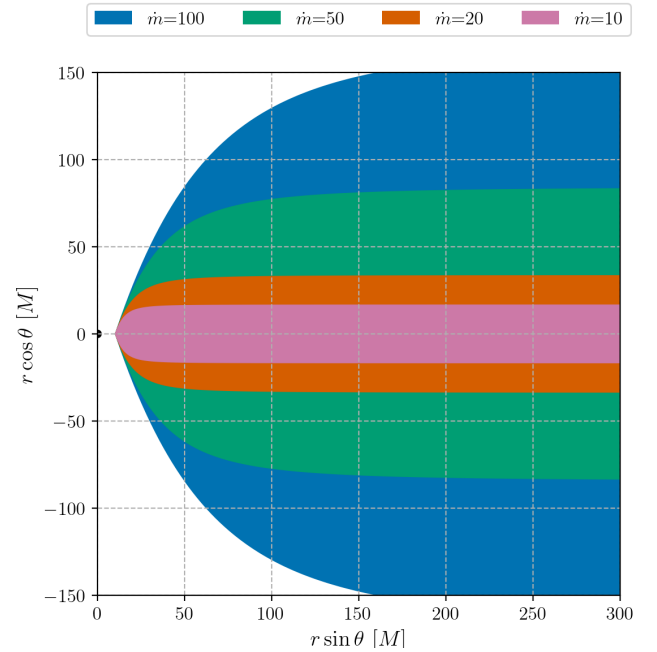


Figure 1. Disk profile obtained from the model for various accretion rates. The accretion rate \dot{m} is in units of \dot{M}_{crit} . The inner edge is set to $10M$. The black region at the origin denotes the event horizon of a Schwarzschild black hole.

2017). The source went into a bright outburst in 2017, with its peak luminosity $> 10^{39}$ erg s⁻¹, far exceeding the Eddington limit for a neutron star (Wilson-Hodge et al. 2018).

We analyze the quasi-simultaneous *NICER* (ObsID 1050390113, 1 November 2017) and *NuSTAR* (ObsID 90302319004, 30 October 2017) observations that have been fitted with the standard thin-disk reflection model in Jaisawal et al. (2019) (see their Fig. 7). We follow the procedure in Jaisawal et al. (2019) to process the *NuSTAR* (FPMA and FPMB) data. The *NICER* data are first processed with `nicerl2` (CALDB v20240206 and geomagnetic data updated to March 2024). The source and background spectral files are then extracted using `nicel3-spect` with the default background model. Spectra are grouped to ensure a minimal counts of 100 for each bin before fitting with `XSPEC` v12.13.0c (Arnaud 1996). Best-fit parameter values and uncertainties (90% confidence level unless otherwise stated) are obtained using χ^2 statistics.

As in Jaisawal et al. (2019), we first fit the *NICER* (1–10 keV) and *NuSTAR* (3–79 keV) data with the model: `constant * tbabs * (bbodyrad + cutoffpl + relxill/relxilllp)`. In this model, the `relxill` and `relxilllp` (García et al. 2014) component represent relativistic reflection from a razor-thin accretion disk, assuming fixed emissivity ($q = 3$) and the corona as a

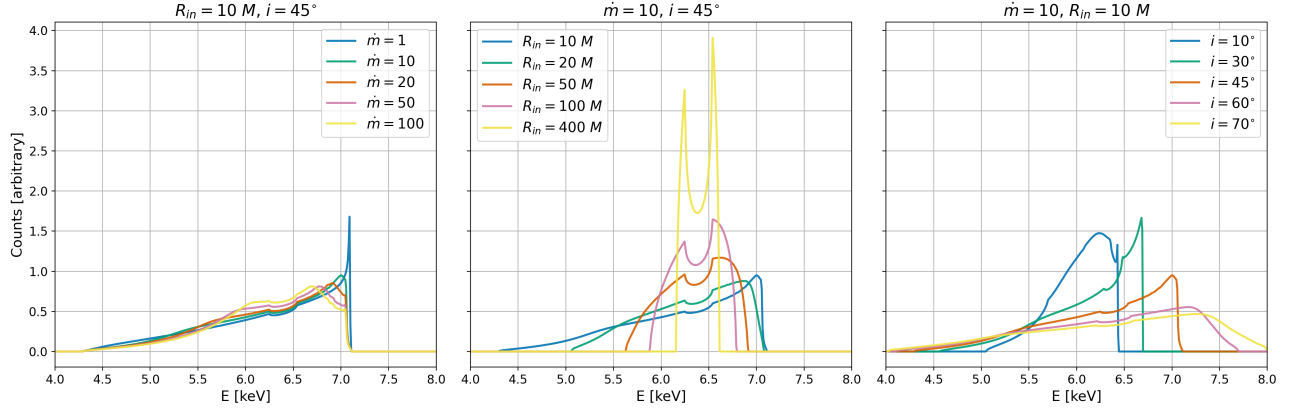


Figure 2. Iron lines obtained from the model for different parameter values. The left panel shows some iron line profiles for different values of the mass accretion rate, the central panel shows some iron line profiles for different values of inner edge of the disk, and the right panel shows some iron line profiles for different values of the disk inclination angle. The other fixed parameter values are on top of every panel. The emissivity index is set to $q_{in} = q_{out} = 3$ in all cases.

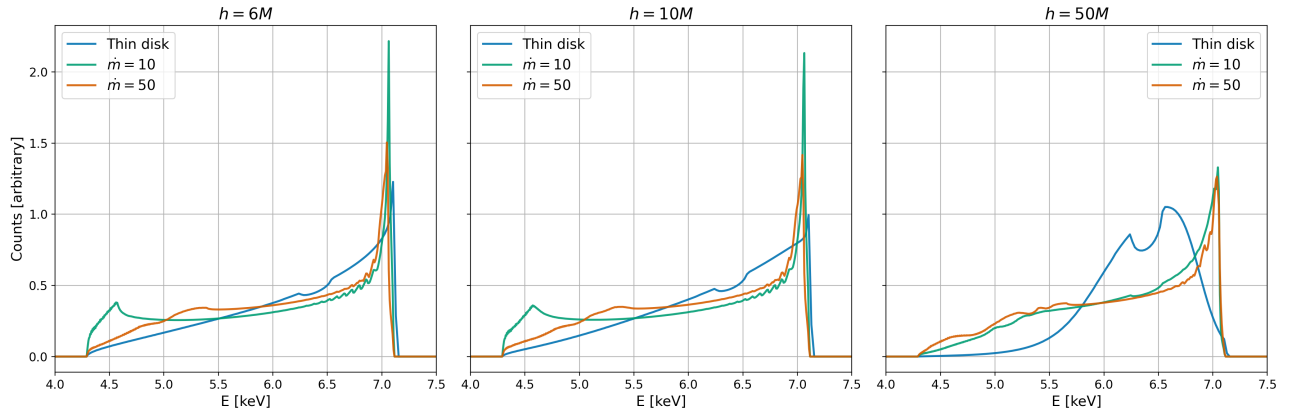


Figure 3. Iron lines obtained from the model for different disk heights using the lamppost emissivity. The left panel shows some iron line profiles for corona height $h = 6M$, the central panel shows iron line profiles for $h = 10M$, and the right panel shows iron line profiles $h = 50M$. The other fixed parameter values are $i = 45^\circ$, $R_{in} = 10M$ and $\Gamma = 2$

| Model | E_{line} | q_{in} | q_{out} | R_{br} | h | \dot{m} | i | R_{in} | R_{out} | z | Γ | $\log \xi$ | A_{Fe} | $\log N_e$ | E_{cut} | kT_e | l | R_f |
|-------------|------------|----------|-----------|----------|-----|-----------|-----|----------|-----------|-----|----------|------------|----------|------------|-----------|--------|-----|-------|
| RELLINESD | ✓ | ✓ | ✓ | ✓ | × | ✓ | ✓ | ✓ | ✓ | ✓ | × | × | × | 15 | × | × | ✓ | × |
| REFLUX | × | ✓ | ✓ | ✓ | × | ✓ | ✓ | ✓ | ✓ | ✓ | ✓ | ✓ | ✓ | 15 | ✓ | × | × | ✓ |
| REFLUXCp | × | ✓ | ✓ | ✓ | × | ✓ | ✓ | ✓ | ✓ | ✓ | ✓ | ✓ | ✓ | 15 | × | ✓ | × | ✓ |
| REFLUXD | × | ✓ | ✓ | ✓ | × | ✓ | ✓ | ✓ | ✓ | ✓ | ✓ | ✓ | ✓ | ✓ | 300 | × | × | ✓ |
| RELLINELFSD | ✓ | × | × | × | ✓ | ✓ | ✓ | ✓ | ✓ | ✓ | ✓ | × | × | 15 | × | × | ✓ | × |
| REFLUXLP | × | × | × | × | ✓ | ✓ | ✓ | ✓ | ✓ | ✓ | ✓ | ✓ | ✓ | 15 | ✓ | × | × | ✓ |
| REFLUXLPCp | × | × | × | × | ✓ | ✓ | ✓ | ✓ | ✓ | ✓ | ✓ | ✓ | ✓ | 15 | × | ✓ | × | ✓ |
| REFLUXLPD | × | × | × | × | ✓ | ✓ | ✓ | ✓ | ✓ | ✓ | ✓ | ✓ | ✓ | ✓ | 300 | × | × | ✓ |

Table 1. Parameter availability for different sub-models. Here, ✓ means the parameter is available in the given sub-model and × means the parameter is not available.

point source above the black hole at a certain height (h), respectively. We fix the spin parameter at $a_* = 0$ and the outer radius of the accretion disk at $1000 M$. The best-fit parameters and the corresponding uncertainties are shown in Tab. 2 for fixed emissivity and in Tab. 3 with lamp-post corona geometry.

At the time of this observation, the mass accretion rate of the source was at super-Eddington level. The absorption corrected X-ray flux in the 0.01-100 keV band is around 10 times of the Eddington limit. Therefore, a thick disk, instead of thin one, is expected. We replace the `relxill/relxilllp` component with our `REFLUX/REFLUXLP` model, with the mass accretion rate fixed at 10 times of the Eddington accretion rate. As shown in Tabs. 2 and 3, the models provide a good fit to the data, with the χ^2 close to that of `relxill/relxilllp`. The best-fit model components and residuals are shown in Fig. 4.

4. DISCUSSIONS

The quality of the fits with the model with `relxill` and the model with `REFLUX` is similar. We fit the same data and the two models have the same number of free parameters, so we can directly compare their χ^2 and the difference is marginal ($\Delta\chi^2 = 1.98$ for fixed emissivity and 9.86 for lamppost). The χ^2 of the best-fit with `relxill` is slightly lower – a possible reason for this could be the smaller parameter grid of `REFLUX` than `relxill` in the FITS file. However, we know that the source was accreting around 10 times of its Eddington limit, so the fit with `REFLUX` appears to be more appropriate for the spectra analyzed. In Tab. 2, the two models provide consistent estimates of the parameters with the exception of the inclination angle of the disk and the iron abundance. The measurements of the inclination angle are $i = 15.1^{+4}_{-2.4}$ deg (`relxill`) and $25.5^{+3}_{-1.7}$ (`REFLUX`). However, the estimates of disk inclination angles inferred from the analysis of reflection features are normally not very accurate and both models suggest a low value of i . Estimates of the iron abundance using X-ray reflection spectroscopy are even more problematic. It is currently unclear why reflection measurements often suggest super-solar iron abundances (but there are also sources for which reflection measurements suggest iron abundances significantly lower than the solar one); see, for instance, [Bambi et al. \(2021\)](#) for a short review on the problem. It may be related to a deficiency of current reflection models (e.g., underestimate of the disk electron density ([Jiang et al. 2019a,b](#); [Liu et al. 2023b](#)), presence of two or more coronae ([Fürst et al. 2015](#)), etc.) or a true physical phenomenon, like radiative levitation of metal ions in the inner part of the ac-

cretion disk ([Reynolds et al. 2012](#)). The estimate of the iron abundance with `REFLUX` would go to the right direction, decreasing the value of A_{Fe} with respect to that inferred with `relxill`, but we would need to analyze more sources and more observations to see if this is a feature of our model and not an accidental result for the spectra analyzed in the previous section. In Tab. 3, we see that for a lamppost geometry, the inclination angle and the iron abundance for both the models closely match the result of `REFLUX` in the analysis with fixed emissivity. However, we see a significant difference in the corona height and the inner edge of the disk. With `relxill`, we see a very low corona height (the lowest in the model) and a larger value for the inner edge. With `REFLUX`, the case is the opposite, we obtain a higher corona height $h > 65M$ and inner edge closer to the central object $R_{in} < 14M$. In the case of `REFLUX`, we see a small norm possibly because the whole disk may not be illuminated for many different h and R_{in} configurations making the flux from the outer part of the disk negligible. We caution the readers against interpreting the high value of $h > 65M$ too rigidly. As in our analysis, we assume a lamppost geometry, which may not be applicable to an Ultra-Luminous Pulsar (ULP) like Swift J0243.6+6124. The system might instead contain a more extended primary illuminating source, such as an accretion column (e.g., [Pinto & Walton \(2023\)](#)). Nonetheless, we observed changes in inferred geometries when a slim disk model was employed. This underscores the critical importance of considering disk geometry when addressing systematic uncertainties. Such uncertainties significantly affect the inferred disk inner radius and, consequently, the magnetic field of ULPs (e.g., [Jaisawal et al. \(2019\)](#)). We will further investigate Swift J0243.6+6124 in this perspective in the future.

A more detailed analysis of the 2017 *NICER* and *NuSTAR* data of Swift J0243.6+6124 is beyond the purpose of the present work, which is the presentation of `REFLUX`. In our fits (with both `relxill` and `REFLUX`), we have assumed that the spectrum illuminating the disk, and responsible for the reflection component can be described by a power law with a high-energy cutoff. However, this may not be the case for Swift J0243.6+6124. A power law with a high-energy cutoff is the spectrum expected for Comptonized photons, which is the case in which thermal photons from an accretion disk can inverse Compton scatter off free electrons in a hot corona. In the case of a neutron star, reflection features may be produced by illumination of the disk by thermal photons from the surface of the neutron star. Such a scenario could be implemented in `REFLUX` by using the `xillverNS`

| Model | Parameter | Unit | Relxill | Reflux |
|-------------------|-----------------|---------------------------|------------------------------|------------------------------|
| Tbabs | nH | 10^{22} cm^{-2} | $0.683^{+0.009}_{-0.011}$ | $0.664^{+0.01}_{-0.006}$ |
| Cutoffpl | Γ | | $1.423^{+0.009}_{-0.009}$ | $1.434^{+0.014}_{-0.009}$ |
| | Ecut | keV | $24.3^{+0.6}_{-0.5}$ | $24.8^{+0.3}_{-0.4}$ |
| | norm | | $12.4^{+0.5}_{-0.5}$ | $12.40^{+0.5}_{-0.29}$ |
| Bbodyrad | kT | keV | $1.213^{+0.019}_{-0.018}$ | $1.234^{+0.009}_{-0.013}$ |
| | norm | | 955^{+21}_{-33} | 988^{+25}_{-27} |
| Reflection | Incl | deg | $15.1^{+4}_{-2.4}$ | $25.5^{+3}_{-1.7}$ |
| | R_{in} | M | 37^{+9}_{-7} | 34^{+8}_{-7} |
| | $\log(\xi)$ | erg cm s^{-1} | $3.54^{+0.05}_{-0.07}$ | $3.29^{+0.03}_{-0.12}$ |
| | A_{Fe} | solar | $4.2^{+1.4}_{-1.2}$ | $2.39^{+0.5}_{-0.27}$ |
| | norm | | $0.050^{+0.007}_{-0.005}$ | $0.0255^{+0.001}_{-0.0017}$ |
| C_{FPMB} | | | $0.9880^{+0.0014}_{-0.0014}$ | $0.9880^{+0.0014}_{-0.0014}$ |
| C_{XTI} | | | $1.242^{+0.012}_{-0.012}$ | $1.240^{+0.01}_{-0.012}$ |
| χ^2/ν | | | 2855.14/2624 | 2857.12/2624 |

Table 2. Best-fit parameters for the model with **relxill** and the model with **REFLUXT**. The reported uncertainties correspond to the 90% interval limits for one relevant parameter ($\Delta\chi^2 = 2.71$).

| Model | Parameter | Unit | Relxillp | Refluxlp |
|-------------------|-----------------|---------------------------|------------------------------|---------------------------------------|
| Tbabs | nH | 10^{22} cm^{-2} | $0.667^{+0.009}_{-0.009}$ | $0.671^{+0.007}_{-0.008}$ |
| Cutoffpl | Γ | | $1.434^{+0.01}_{-0.009}$ | $1.438^{+0.008}_{-0.01}$ |
| | Ecut | keV | $24.74^{+0.26}_{-0.4}$ | $24.7^{+0.3}_{-0.3}$ |
| | norm | | $12.4^{+0.4}_{-0.3}$ | $12.6^{+0.3}_{-0.3}$ |
| Bbodyrad | kT | keV | $1.23^{+0.01}_{-0.01}$ | $1.235^{+0.005}_{-0.006}$ |
| | norm | | 1000^{+40}_{-30} | 970^{+30}_{-25} |
| Reflection | h | M | $2.20^{+0.07}_{-P}$ | > 65 |
| | Incl | deg | $25.7^{+2.7}_{-1.3}$ | $26.5^{+1.2}_{-2.4}$ |
| | R_{in} | M | 39^{+9}_{-8} | < 14 |
| | $\log(\xi)$ | erg cm s^{-1} | $3.31^{+0.04}_{-0.05}$ | $3.284^{+0.029}_{-0.07}$ |
| | A_{Fe} | solar | $2.4^{+0.3}_{-0.3}$ | $2.6^{+0.4}_{-0.3}$ |
| | norm | | $3.58^{+0.24}_{-0.7}$ | $1.37^{+0.10}_{-0.06} \times 10^{-7}$ |
| C_{FPMB} | | | $0.9880^{+0.0014}_{-0.0014}$ | $0.9880^{+0.0014}_{-0.0014}$ |
| C_{XTI} | | | $1.223^{+0.012}_{-0.013}$ | $1.238^{+0.011}_{-0.01}$ |
| χ^2/ν | | | 2816.49/2623 | 2826.35/2623 |

Table 3. Best-fit parameters for the model with **relxillp** and the model with **REFLUXLP**. The reported uncertainties correspond to the 90% interval limits for one relevant parameter ($\Delta\chi^2 = 2.71$).

table, in which reflection spectra are produced by an incident blackbody spectrum.

While for neutron star XRBs like Swift J0243.6+6124 the Schwarzschild metric should describe well the space-time geometry around the source, in the case of other super-Eddington X-ray sources (black hole XRBs, AGNs, and TDEs) deviations from the Schwarzschild background can be important and it will be necessary to implement the Kerr metric in **REFLUX**. This is also left to future work.

This work was supported by the National Natural Science Foundation of China (NSFC), Grant No. 12250610185 and 12261131497, and the Natural Science Foundation of Shanghai, Grant No. 22ZR1403400. J.J. acknowledges support from Leverhulme Trust, Isaac Newton Trust and St Edmund’s College, University of Cambridge.

Facilities: Swift, NICER, NuSTAR

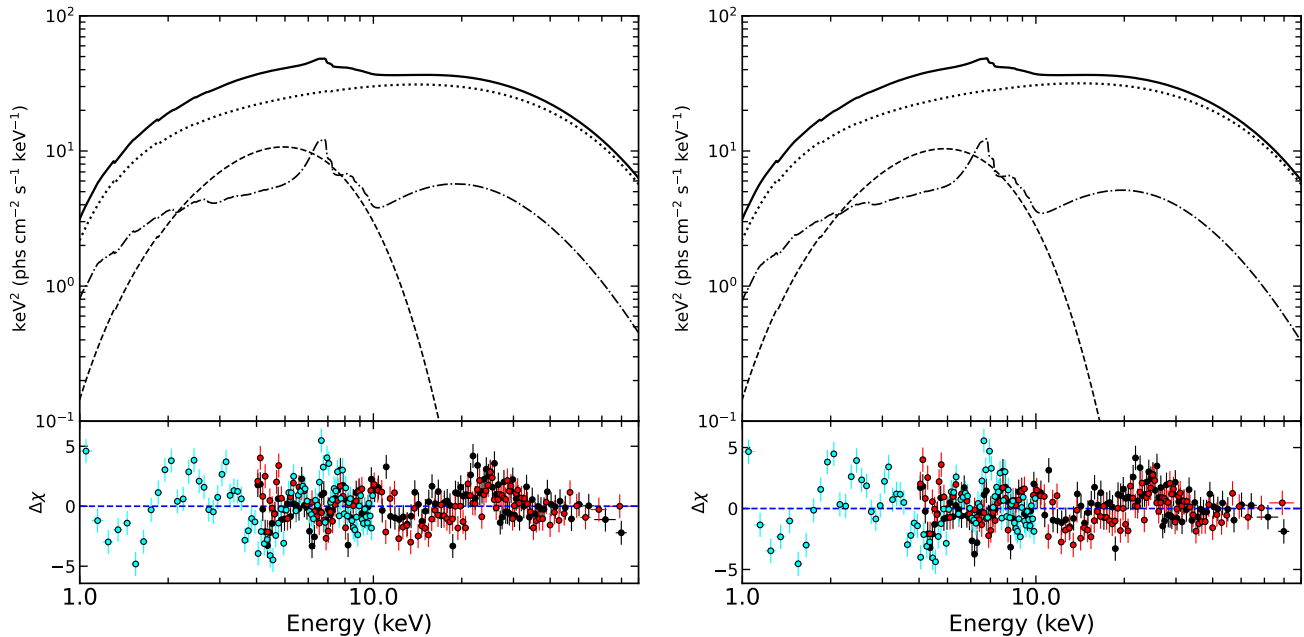


Figure 4. Best-fit model components and residuals for the lamppost geometry (left) and the power-law emissivity profile (right) with the **REFLUX** model. The black and red colors represent data of FPMA and FPMB, respectively. *NICER* data are plotted in cyan. Data are rebinned for visual clarity.

Software: astropy (Astropy Collaboration et al. 2013, 2018), XSPEC (Arnaud 1996), numpy (Harris et al. 2020), scipy (Virtanen et al. 2020), matplotlib (Hunter

2007), raytransfer (Abdikamalov et al. 2024a), blackray (Abdikamalov et al. 2024b), blacklamp (Abdikamalov et al. 2024c)

REFERENCES

- Abdikamalov, A., Ayzenberg, D., Bambi, C., et al. 2024a, raytransfer, v1.0.0, Zenodo, doi: [10.5281/zenodo.12703492](https://doi.org/10.5281/zenodo.12703492)
- Abdikamalov, A. B., Ayzenberg, D., Bambi, C., et al. 2019, *Astrophys. J.*, 878, 91, doi: [10.3847/1538-4357/ab1f89](https://doi.org/10.3847/1538-4357/ab1f89)
- . 2020, *Astrophys. J.*, 899, 80, doi: [10.3847/1538-4357/aba625](https://doi.org/10.3847/1538-4357/aba625)
- . 2024b, blackray, v1.0.1, Zenodo, doi: [10.5281/zenodo.10673859](https://doi.org/10.5281/zenodo.10673859)
- . 2024c, blacklamp, v1.0.0, Zenodo, doi: [10.5281/zenodo.10673757](https://doi.org/10.5281/zenodo.10673757)
- Arnaud, K. A. 1996, in *Astronomical Society of the Pacific Conference Series*, Vol. 101, *Astronomical Data Analysis Software and Systems V*, ed. G. H. Jacoby & J. Barnes, 17
- Astropy Collaboration, Robitaille, T. P., Tollerud, E. J., et al. 2013, *A&A*, 558, A33, doi: [10.1051/0004-6361/201322068](https://doi.org/10.1051/0004-6361/201322068)
- Astropy Collaboration, Price-Whelan, A. M., Sipőcz, B. M., et al. 2018, *AJ*, 156, 123, doi: [10.3847/1538-3881/aabc4f](https://doi.org/10.3847/1538-3881/aabc4f)
- Bambi, C. 2017, *Black Holes: A Laboratory for Testing Strong Gravity* (Springer Singapore), doi: [10.1007/978-981-10-4524-0](https://doi.org/10.1007/978-981-10-4524-0)
- Bambi, C., Cardenas-Avendano, A., Dauser, T., Garcia, J. A., & Nampalliwar, S. 2017, *Astrophys. J.*, 842, 76, doi: [10.3847/1538-4357/aa74c0](https://doi.org/10.3847/1538-4357/aa74c0)
- Bambi, C., Brenneman, L. W., Dauser, T., et al. 2021, *SSRv*, 217, 65, doi: [10.1007/s11214-021-00841-8](https://doi.org/10.1007/s11214-021-00841-8)
- Bhattacharyya, S., & Strohmayer, T. E. 2007, *ApJL*, 664, L103, doi: [10.1086/520844](https://doi.org/10.1086/520844)
- Bloom, J. S., Giannios, D., Metzger, B. D., et al. 2011, *Science*, 333, 203, doi: [10.1126/science.1207150](https://doi.org/10.1126/science.1207150)
- Brenneman, L. W., & Reynolds, C. S. 2006, *ApJ*, 652, 1028, doi: [10.1086/508146](https://doi.org/10.1086/508146)
- Burrows, D. N., Kennea, J. A., Ghisellini, G., et al. 2011, *Nature*, 476, 421, doi: [10.1038/nature10374](https://doi.org/10.1038/nature10374)
- Caballero-Garcia, M. D., Bursa, M., Dovciak, M., et al. 2017, *Contrib. Astron. Obs. Skalnaté Pleso*, 47, 84. <https://arxiv.org/abs/1705.07859>
- Cackett, E. M., Miller, J. M., Bhattacharyya, S., et al. 2008, *ApJ*, 674, 415, doi: [10.1086/524936](https://doi.org/10.1086/524936)

- Cao, Z., Nampalliwar, S., Bambi, C., Dauser, T., & García, J. A. 2018, *PhRvL*, 120, 051101, doi: [10.1103/PhysRevLett.120.051101](https://doi.org/10.1103/PhysRevLett.120.051101)
- Cenko, S. B., Barthelmy, S. D., D’Avanzo, P., et al. 2017, GRB Coordinates Network, 21960, 1
- Cunningham, C. T. 1975, *Astrophys. J.*, 202, 788, doi: [10.1086/154033](https://doi.org/10.1086/154033)
- Dauser, T., Wilms, J., Reynolds, C. S., & Brenneman, L. W. 2010, *Mon. Not. Roy. Astron. Soc.*, 409, 1534, doi: [10.1111/j.1365-2966.2010.17393.x](https://doi.org/10.1111/j.1365-2966.2010.17393.x)
- Draghis, P. A., Miller, J. M., Zoghbi, A., et al. 2023, *ApJ*, 946, 19, doi: [10.3847/1538-4357/acafe7](https://doi.org/10.3847/1538-4357/acafe7)
- Fabian, A. C., Rees, M. J., Stella, L., & White, N. E. 1989, *Mon. Not. Roy. Astron. Soc.*, 238, 729, doi: [10.1093/mnras/238.3.729](https://doi.org/10.1093/mnras/238.3.729)
- Fabrika, S. N., Atapin, K. E., Vinokurov, A. S., & Sholukhova, O. N. 2021, *Astrophysical Bulletin*, 76, 6, doi: [10.1134/S1990341321010077](https://doi.org/10.1134/S1990341321010077)
- Fan, X., Bañados, E., & Simcoe, R. A. 2023, *ARA&A*, 61, 373, doi: [10.1146/annurev-astro-052920-102455](https://doi.org/10.1146/annurev-astro-052920-102455)
- Fürst, F., Nowak, M. A., Tomsick, J. A., et al. 2015, *ApJ*, 808, 122, doi: [10.1088/0004-637X/808/2/122](https://doi.org/10.1088/0004-637X/808/2/122)
- García, J., Dauser, T., Reynolds, C. S., et al. 2013, *ApJ*, 768, 146, doi: [10.1088/0004-637X/768/2/146](https://doi.org/10.1088/0004-637X/768/2/146)
- García, J., Dauser, T., Lohfink, A., et al. 2014, *ApJ*, 782, 76, doi: [10.1088/0004-637X/782/2/76](https://doi.org/10.1088/0004-637X/782/2/76)
- Gezari, S. 2021, *Ann. Rev. Astron. Astrophys.*, 59, 21, doi: [10.1146/annurev-astro-111720-030029](https://doi.org/10.1146/annurev-astro-111720-030029)
- Harris, C. R., et al. 2020, *Nature*, 585, 357, doi: [10.1038/s41586-020-2649-2](https://doi.org/10.1038/s41586-020-2649-2)
- Hunter, J. D. 2007, *Computing in Science & Engineering*, 9, 90, doi: [10.1109/MCSE.2007.55](https://doi.org/10.1109/MCSE.2007.55)
- Jaisawal, G. K., Wilson-Hodge, C. A., Fabian, A. C., et al. 2019, *ApJ*, 885, 18, doi: [10.3847/1538-4357/ab4595](https://doi.org/10.3847/1538-4357/ab4595)
- Jiang, J., Abdikamalov, A. B., Bambi, C., & Reynolds, C. S. 2022, *Mon. Not. Roy. Astron. Soc.*, 514, 3246, doi: [10.1093/mnras/stac1369](https://doi.org/10.1093/mnras/stac1369)
- Jiang, J., Fabian, A. C., Wang, J., et al. 2019a, *MNRAS*, 484, 1972, doi: [10.1093/mnras/stz095](https://doi.org/10.1093/mnras/stz095)
- Jiang, J., Fabian, A. C., Dauser, T., et al. 2019b, *MNRAS*, 489, 3436, doi: [10.1093/mnras/stz2326](https://doi.org/10.1093/mnras/stz2326)
- Kaaret, P., Feng, H., & Roberts, T. P. 2017, *Ann. Rev. Astron. Astrophys.*, 55, 303, doi: [10.1146/annurev-astro-091916-055259](https://doi.org/10.1146/annurev-astro-091916-055259)
- Kara, E., Dai, L., Reynolds, C. S., & Kallman, T. 2018, *Mon. Not. Roy. Astron. Soc.*, 474, 3593, doi: [10.1093/mnras/stx3004](https://doi.org/10.1093/mnras/stx3004)
- Kara, E., Miller, J. M., Reynolds, C., & Dai, L. 2016, *Nature*, 535, 388, doi: [10.1038/nature18007](https://doi.org/10.1038/nature18007)
- Kawaguchi, T. 2003, *Astrophys. J.*, 593, 69, doi: [10.1086/376404](https://doi.org/10.1086/376404)
- Kennea, J. A., Lien, A. Y., Krimm, H. A., Cenko, S. B., & Siegel, M. H. 2017, *The Astronomer’s Telegram*, 10809, 1
- Lanzuisi, G., et al. 2016, *Astron. Astrophys.*, 590, A77, doi: [10.1051/0004-6361/201628325](https://doi.org/10.1051/0004-6361/201628325)
- Lin, D., Maksym, P. W., Irwin, J. A., et al. 2015, *Astrophys. J.*, 811, 43, doi: [10.1088/0004-637X/811/1/43](https://doi.org/10.1088/0004-637X/811/1/43)
- Liu, H., Bambi, C., Jiang, J., et al. 2023a, *ApJ*, 950, 5, doi: [10.3847/1538-4357/acca17](https://doi.org/10.3847/1538-4357/acca17)
- Liu, H., Jiang, J., Zhang, Z., et al. 2023b, *ApJ*, 951, 145, doi: [10.3847/1538-4357/acd8b9](https://doi.org/10.3847/1538-4357/acd8b9)
- Massoneau, W., Volonteri, M., Dubois, Y., & Beckmann, R. S. 2023, *A&A*, 670, A180, doi: [10.1051/0004-6361/202243170](https://doi.org/10.1051/0004-6361/202243170)
- Matthee, J., et al. 2024, *Astrophys. J.*, 963, 129, doi: [10.3847/1538-4357/ad2345](https://doi.org/10.3847/1538-4357/ad2345)
- Mortlock, D. J., et al. 2011, *Nature*, 474, 616, doi: [10.1038/nature10159](https://doi.org/10.1038/nature10159)
- Motta, S. E., et al. 2017, *Mon. Not. Roy. Astron. Soc.*, 471, 1797, doi: [10.1093/mnras/stx1699](https://doi.org/10.1093/mnras/stx1699)
- Nandra, K., O’Neill, P. M., George, I. M., & Reeves, J. N. 2007, *MNRAS*, 382, 194, doi: [10.1111/j.1365-2966.2007.12331.x](https://doi.org/10.1111/j.1365-2966.2007.12331.x)
- Novikov, I. D., & Thorne, K. S. 1973, in *Black Holes (Les Astres Occlus)*, 343–450
- Page, D. N., & Thorne, K. S. 1974, *Astrophys. J.*, 191, 499, doi: [10.1086/152990](https://doi.org/10.1086/152990)
- Pinto, C., & Walton, D. J. 2023. <https://arxiv.org/abs/2302.00006>
- Reynolds, C. S., Brenneman, L. W., Lohfink, A. M., et al. 2012, *ApJ*, 755, 88, doi: [10.1088/0004-637X/755/2/88](https://doi.org/10.1088/0004-637X/755/2/88)
- Riaz, S., Ayzenberg, D., Bambi, C., & Nampalliwar, S. 2020a, *Mon. Not. Roy. Astron. Soc.*, 491, 417, doi: [10.1093/mnras/stz3022](https://doi.org/10.1093/mnras/stz3022)
- . 2020b, *Astrophys. J.*, 895, 61, doi: [10.3847/1538-4357/ab89ab](https://doi.org/10.3847/1538-4357/ab89ab)
- Ross, R. R., & Fabian, A. C. 2005, *MNRAS*, 358, 211, doi: [10.1111/j.1365-2966.2005.08797.x](https://doi.org/10.1111/j.1365-2966.2005.08797.x)
- Sadowski, A. 2011, *arXiv e-prints*, arXiv:1108.0396, doi: [10.48550/arXiv.1108.0396](https://doi.org/10.48550/arXiv.1108.0396)
- Shashank, S., Riaz, S., Abdikamalov, A. B., & Bambi, C. 2022, *Astrophys. J.*, 938, 53, doi: [10.3847/1538-4357/ac9128](https://doi.org/10.3847/1538-4357/ac9128)
- Speith, R., Riffert, H., & Ruder, H. 1995, *Computer Physics Communications*, 88, 109, doi: [10.1016/0010-4655\(95\)00067-P](https://doi.org/10.1016/0010-4655(95)00067-P)
- Tanaka, Y., Nandra, K., Fabian, A. C., et al. 1995, *Nature*, 375, 659, doi: [10.1038/375659a0](https://doi.org/10.1038/375659a0)

- Taylor, C., & Reynolds, C. S. 2018, *Astrophys. J.*, 855, 120, doi: [10.3847/1538-4357/aaad63](https://doi.org/10.3847/1538-4357/aaad63)
- Tripathi, A., Abdikamalov, A. B., Ayzenberg, D., Bambi, C., & Liu, H. 2021, *Astrophys. J.*, 913, 129, doi: [10.3847/1538-4357/abf6c5](https://doi.org/10.3847/1538-4357/abf6c5)
- Tripathi, A., Nampalliwar, S., Abdikamalov, A. B., et al. 2019, *ApJ*, 875, 56, doi: [10.3847/1538-4357/ab0e7e](https://doi.org/10.3847/1538-4357/ab0e7e)
- Tripathi, A., Zhang, Y., Abdikamalov, A. B., et al. 2021, *ApJ*, 913, 79, doi: [10.3847/1538-4357/abf6cd](https://doi.org/10.3847/1538-4357/abf6cd)
- Tsai, C.-W., Eisenhardt, P. R. M., Jun, H. D., et al. 2018, *ApJ*, 868, 15, doi: [10.3847/1538-4357/aae698](https://doi.org/10.3847/1538-4357/aae698)
- Veledina, A., et al. 2023. <https://arxiv.org/abs/2303.01174>
- Virtanen, P., Gommers, R., Oliphant, T. E., et al. 2020, *Nature Methods*, 17, 261, doi: [10.1038/s41592-019-0686-2](https://doi.org/10.1038/s41592-019-0686-2)
- Walton, D. J., Nardini, E., Fabian, A. C., Gallo, L. C., & Reis, R. C. 2013, *MNRAS*, 428, 2901, doi: [10.1093/mnras/sts227](https://doi.org/10.1093/mnras/sts227)
- Watarai, K. 2006, *Astrophys. J.*, 648, 523, doi: [10.1086/505854](https://doi.org/10.1086/505854)
- Wen, S., Jonker, P. G., Stone, N. C., Zabludoff, A. I., & Cao, Z. 2022, *Astrophys. J.*, 933, 31, doi: [10.3847/1538-4357/ac70c5](https://doi.org/10.3847/1538-4357/ac70c5)
- Wilson-Hodge, C. A., Malacaria, C., Jenke, P. A., et al. 2018, *ApJ*, 863, 9, doi: [10.3847/1538-4357/aace60](https://doi.org/10.3847/1538-4357/aace60)
- Yao, Y., Lu, W., Guolo, M., et al. 2022, *ApJ*, 937, 8, doi: [10.3847/1538-4357/ac898a](https://doi.org/10.3847/1538-4357/ac898a)
- Yao, Y., Guolo, M., Tombesi, F., et al. 2024, arXiv e-prints, arXiv:2405.11343, doi: [10.48550/arXiv.2405.11343](https://doi.org/10.48550/arXiv.2405.11343)
- Zdziarski, A. A., Johnson, W. N., & Magdziarz, P. 1996, *MNRAS*, 283, 193, doi: [10.1093/mnras/283.1.193](https://doi.org/10.1093/mnras/283.1.193)
- Zhang, Z., Thomsen, L. L., Dai, L., et al. 2024. <https://arxiv.org/abs/2407.08596>
- Życki, P. T., Done, C., & Smith, D. A. 1999, *MNRAS*, 309, 561, doi: [10.1046/j.1365-8711.1999.02885.x](https://doi.org/10.1046/j.1365-8711.1999.02885.x)